Self-Propelled Particle Model for Cell-Sorting Phenomena

Julio M. Belmonte,[1] Gilberto L. Thomas,[1] Leonardo G. Brunnet,[1] Rita M. C. de Almeida,[1] and Hugues Chaté[2]

[1]*Instituto de Física, Universidade Federal do Rio Grande do Sul, Avenida Bento Gonçalves, 9500, P.B. 15051, 91501-970 Porto Alegre, Brazil*

[2]*CEA—Service de Physique de l'État Condensé, CEN Saclay, 91191 Gif-sur-Yvette, France*

(Received 15 October 2007; published 20 June 2008)

A self-propelled particle model is introduced to study cell sorting occurring in some living organisms. This allows us to evaluate the influence of intrinsic cell motility separately from differential adhesion with fluctuations, a mechanism previously shown to be sufficient to explain a variety of cell rearrangement processes. We find that the tendency of cells to actively follow their neighbors greatly reduces segregation time scales. A finite-size analysis of the sorting process reveals clear algebraic growth laws as in physical phase-ordering processes, albeit with unusual scaling exponents.

DOI: 10.1103/PhysRevLett.100.248702 PACS numbers: 87.17.−d, 05.65.+b, 64.75.−g

Regeneration after tissue dissociation and reaggregation of some species of sponges, sea urchins, and hydras has been investigated in a series of experiments [1]. These phenomena involve cell sorting: Initially mixed cells form clusters, similarly to domain growth processes in physics. To explain cell sorting, Steinberg [2] proposed the differential adhesion hypothesis (DAH), which postulates that local rearrangements depend on the adhesion and motility properties of the different types of cells involved.

Experiments have verified some of the DAH postulates. Surface tension measurements in chicken embryonic tissues [3] and determination of adhesive forces between pairs of *Hydra* cells [4] confirmed the relative magnitudes necessary to favor tissue envelopment: Ectodermic cells are less cohesive than endodermic cells. It was also shown that random membrane ruffling induces effective cell motion [5]. However, the coherent component of cellular flow must also be considered, as in viscoelastic fluids [6]. Remarkable experiments on *Hydra* performed in two spatial dimensions by Rieu *et al.* [7,8] discriminate between random and coherent motion contributions to cell segregation, showing that, during aggregate rounding or sorting, endodermic cell dynamics is dominated by the coherent behavior of ectodermic cells. Also, short-range spatial correlations corresponding to parallel displacement of adjacent cells were observed. The diffusive properties of cells were also measured. In all cases, diffusion was found to be normal only beyond a trapping time during which cells keep the same neighbors. This time is smaller for endodermic cells immersed in the ectoderm.

Cell-sorting phenomena, such as *Hydra* regeneration from random cellular aggregates, have been simulated in the seminal work by Graner and Glazier in 1992 [9], later extended by Hogeweg and co-workers [10] (hereafter the GGH model). In the GGH model, cells are represented on a site-labeled lattice. A connected group of sites with the same label stands for a cell, and an energy function accounts for surface tension between adjacent cells while keeping the cell sizes fluctuating around specified targets. Monte Carlo simulations showed that sorting may occur, with less adhesive cells engulfing the more adhesive ones. However, this type of approach cannot easily account for locally coherent active cell motion (see [11] for such an attempt). Moreover, if GGH-like models do lead to realistic final configurations, the simulations performed so far [9] suggest that the growth process underlying cell sorting exhibit slow logarithmic laws at odds with the experimental work of Ref. [12], which advocates linear growth, although these measurements were performed over times too short to be fully conclusive. There are some other interesting approaches to model cell sorting, but the segregation evolution is not quantitatively measured [13].

Here we introduce a simple, versatile, self-propelled particle model for cell sorting and other situations where cohesive cells actively move. While incorporating the basic tenets of DAH, it allows for an independent assessment of the role played by coherent active motion using particles interacting through velocity-dependent forces. We find that even a moderate amount of local coherent motion considerably speeds up cell sorting. We show that cell cluster growth, in our model, is characterized by algebraic scaling laws with unusual exponents. Moreover, our results hint that the logarithmic scaling found in the GGH model might be valid only in the absence of any coherent active motion.

Self-propelled particle systems have been used as models for the collective motion of animals [14], for active cell motion in bacterial baths [15], bacteria and amoeba colonies [16], or groups of cells moving on a substrate such as keratocytes [17] and melanocytes [18]. The Vicsek model [19] is probably the simplest model of active motion: Point particles move in a continuous space at fixed speed, locally aligning with their neighbors. However, as such, the particles have no ''physical size'' and no cohesive interactions, both ingredients needed when modeling cell sorting. Grégoire *et al.* extended the Vicsek model by considering a classic two-body attraction or repulsion force [20,21]. They showed that this allows for cohesion while endowing the particles with a well-defined but fluctuating size. Our

cell-sorting model is an extension of this work where we consider two cell types with different interaction intensities to simulate differential adhesion.

Consider N particles moving with velocities of fixed modulus v_0 (driven-overdamped dynamics). In two space dimensions, the state of particle n at time t is represented by its position $\mathbf{x}_n^t$ and a single orientation angle θ_n^t (or, equivalently, by its velocity $\mathbf{v}_n^t$). At every time step ($\Delta t = 1$ without loss of generality), we calculate the new orientation θ_n^{t+1} of each particle along which it is displaced by a distance v_0. The positions and orientations of all neighboring particles m within a radius r_0 of particle n determine θ_n^{t+1} according to

$$\theta_n^{t+1} = \arg\left[\sum_{m\sim n}\left(\alpha_{nm}\frac{\mathbf{v}_m^t}{v_0} + \beta_{nm} f_{nm}^t \mathbf{e}_{nm}^t\right) + \eta \mathbf{u}_n^t\right], \quad (1)$$

where $f_{nm}^t \mathbf{e}_{nm}^t$ is the force exerted by particle m on particle n, along the direction $\mathbf{e}_{nm}^t$ going from particle m to particle n, and $\mathbf{u}_n^t$ is a unit vector with random, uniformly distributed orientation. Parameters α_{nm} and β_{nm} control, respectively, the relative weights of the alignment interaction (first term) and of the radial two-body forces f_{nm}, with respect to the noise intensity η. (In the following, $\eta = 1$, without loss of generality.) The radial force consists of a hard core repulsion for distances smaller than a core radius r_c and a harmoniclike interaction around the equilibrium radius r_e, from r_c up to a maximum range r_0:

$$f_{nm} = \begin{cases} \infty & \text{if } r_{nm} < r_c, \\ 1 - \frac{r_{nm}}{r_e} & \text{if } r_c < r_{nm} < r_0, \\ 0 & \text{if } r_{nm} > r_0. \end{cases} \quad (2)$$

All distances are expressed in units of r_e, i.e., $r_e = 1$. In this case, $r_0 = 1.32 r_e$ is chosen such that each particle has six neighbors on average. The remaining parameters are $r_c = 0.40 r_e$ and $v_0 = 0.1 r_e$.

By considering all cells of the same type, such that $\alpha_{mn} = \alpha$ and $\beta_{mn} = \beta$, we find a (α, β) phase diagram qualitatively similar to that reported in Ref. [20]: gas phase at low enough β values and liquid and solidlike phases as β is increased. For large-enough α values, the liquid and solid phases are endowed with long-range orientational order, i.e., active collective motion sets in. These latter regimes are not realistic in the context of cell sorting, and we limit ourselves to small α values for which no long-range collective motion arises. As β is increased, cohesion increases, eventually inducing two regimes for the diffusive properties of particles: At short times, particles are trapped by their neighbors, but beyond this trapping time τ, diffusion is normal.

Differential adhesion is described by different β values associated to interaction between cells of different types. For simplicity, we choose a uniform value of α for all cells. Having *Hydra* in mind (detailed experimental data are available), we define two kinds of particles, 1 and 2, corresponding, respectively, to endodermic and ectodermic cell types. The interaction parameters are thus: β_{11} and β_{22} to account for cell cohesion within each cell type and β_{21} and β_{12} for intercell-type interactions, assumed for simplicity to be symmetric, i.e., $\beta_{12} = \beta_{21}$.

Our simulations were performed on a square domain of linear size L much larger than the typical surface occupied by cells: $L^2 \gg N\pi r_e^2$. Initially, the particles are randomly placed in a square subdomain of linear size ℓ ($\ell \times \ell \simeq N\pi r_e^2$). The simulation starts with all cells possessing ectoderm attributes ($\beta_{22} = 2.5$, in the liquid phase), until they form a compact group. The duration of this phase depends on N ($\sim$4000 time steps for $N = 800$). We then randomly label a fraction of cells as ''endodermic'' and fix the two-body interaction parameters as $\beta_{11} = 3.83$, $\beta_{12} = 2.53$, and $\beta_{22} = 2.5$. For $\beta_{11} = 3.83$, the trapping time τ is of the order of 10^4 time steps while it is of order 10 for $\beta < 2.67$, respecting the experimental fact observed in *Hydra* experiments [8] that τ is smaller in pure ectoderm than in pure endoderm.

Figure 1 shows the typical evolution, for $\alpha = 0.01$, of a group of 800 cells with a proportion of 1:3 of endodermic to ectodermic cells (in agreement with experiments on *Hydra*). Figure 1(a) shows the initial, compact cluster. Figure 1(b) is a snapshot 3000 steps later, when small clusters of endodermic cells have formed. Growth continues [Fig. 1(c), $t = 3 \times 10^5$] until a single cluster is formed [Fig. 1(d), $t = 2 \times 10^6$]. The final shape is never perfectly round, and some isolated endodermic cells remain in the ectoderm tissue, in agreement with experiments [7].

To quantify the degree of cell sorting, we measure γ_1 (γ_2), defined as the average fraction of ectodermic (endodermic) neighbors around endodermic (ectodermic) cells:

$$\gamma_i = \left\langle \frac{n_{\neq}}{n_{=} + n_{\neq}} \right\rangle, \quad (3)$$

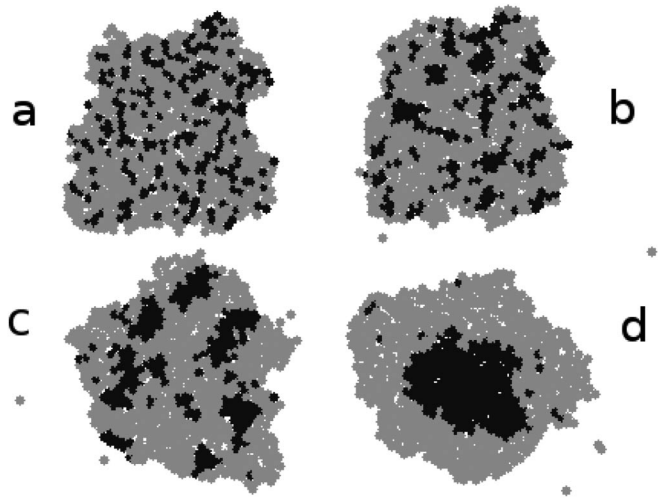

FIG. 1. Sorting of 800 cells. Black and gray circles represent, respectively, endodermic and ectodermic cells. (a) Initial configuration; (b) $t = 3 \times 10^3$; (c) $t = 3 \times 10^5$; (d) $t = 2 \times 10^7$.

where $n_{\neq}$ and $n_{=}$ are the numbers of different- and same-type neighbors of a central endodermic ($i = 1$) or ectodermic ($i = 2$) cell. Perfect cell sorting is expected to approach $\gamma_i = 0$ in large systems. In the segregated phase, γ_i is proportional to the total length of interfaces between the clusters. In practice, dispersed cells, effects of noise and disorder, and remaining interfaces prevent γ_i from reaching zero in finite systems.

Figure 2 presents the evolution of γ_1 for several values of α smaller than 0.04, the onset of collective motion (results for γ_2 are similar). A short transient of about 10^4 time steps is observed in all cases. For the larger values ($\alpha = 0.01$, 0.0125, and 0.015), clear algebraic decay is observed after this initial transient, with an exponent $\lambda = 0.18 \pm 0.02$. For smaller α values, logarithmic decay occurs first after the 10^4 transient, followed by a crossover to an algebraic regime with approximately the same power law as for larger α values. The crossover time increases as α decreases and could be infinite for $\alpha = 0$.

For a finite system, the algebraic decay of γ_1 is followed by a saturation at an α- and N-dependent level (see the $\alpha = 0.015$ curve in Fig. 2). For $\alpha = 0.01$–0.015, segregation is efficient, stable, and fast [Fig. 1(d)]. For lower values ($\alpha = 0$ and $\alpha = 0.005$), it takes nearly 1 order of magnitude longer to form a single cluster. For $\alpha > 0.015$, cell sorting is fast, but the coherent motion of subgroups of cells induces strong fluctuations on the central cluster surface, leading sometimes to partial breakup.

During real regeneration phenomena, cells have a finite time to reorder, and the sorting process may end up incomplete. For example, due to an excess in number, cells may die before reaching their correct position, or, because of a too small number of cells, large fluctuations may render the tissues interface unstable [7]. Thus, the regeneration time scale, its relation with the number of cells, and the degree of regeneration achieved are relevant to the organism survival. We now pay attention to these quantities within our model. In what follows, we use, for numerical ease, $\alpha = 0.01$, which yields reasonably fast segregation together with weak interface roughening.

Figure 3(a) (inset) shows cell-sorting evolution for different system sizes N. While the decay exponent λ remains the same, both the asymptotic segregation values γ_1^* and the saturation time t^* scale with N, yielding $\gamma_1^* \sim N^{-\mu}$ and $t^* \sim N^{\nu}$, with $\mu = 0.32 \pm 0.01$ and $\nu = 1.77 \pm 0.04$ [Figs. 3(b) and 3(c)]. Usual scaling arguments imply that $\mu \sim \lambda\nu$ [22]. We estimated $\lambda\nu = 0.32 \pm 0.04$, very close to the measured value of μ. A final check of the scaling analysis above is the collapse plot presented in Fig. 3(a).

The above scaling laws are robust. For example, by changing from $\beta_{11} = 3.83$ to $\beta_{11} = 5$ (much more cohesive core), we find that $\lambda = 0.20 \pm 0.02$. By modifying the displacement rule to one in which the particle displacement is proportional to the resultant "force" [i.e., the quantity

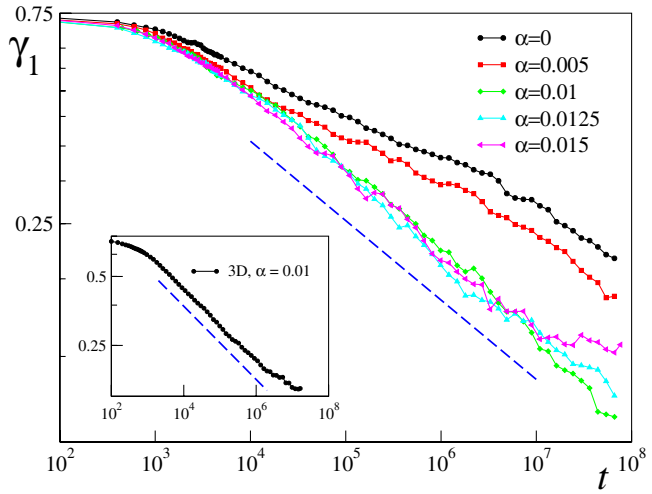

FIG. 2 (color online). Cell sorting in two dimensions from a random, roughly circular initial aggregate of $N = 6400$ cells in a proportion of 1:3 endodermic to ectodermic cells. Evolution of γ_1 for different α values. The dashed line has slope $-\lambda = -0.18$. Inset: Same in three dimensions but with $\alpha = 0.01$ and $\beta_{11} = 8.3$. The dashed line has slope -0.16.

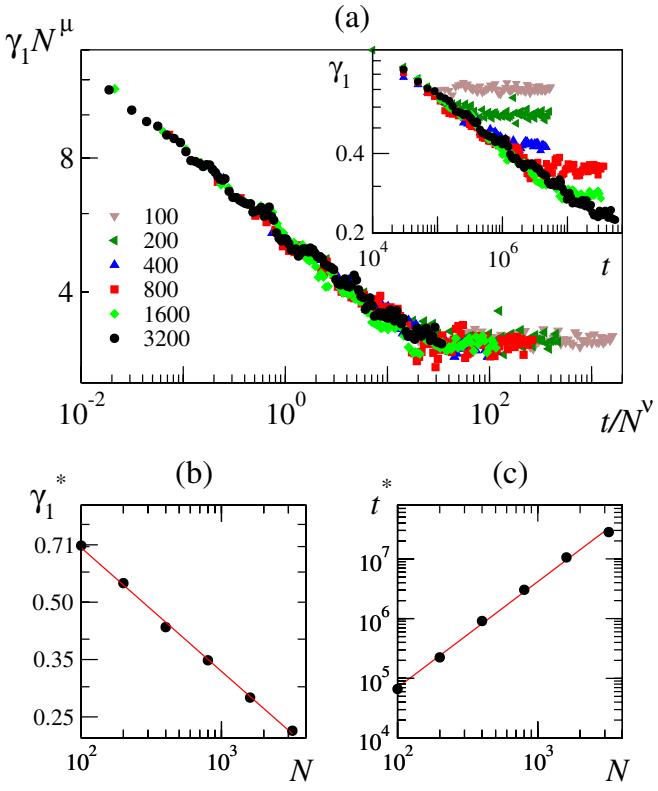

FIG. 3 (color online). (a) Rescaling of the segregation evolution for different total numbers of cells. The raw data are shown in the inset with the same symbol convention. Parameters: $\beta_{11} = 3.83$, $\beta_{12} = 2.53$, $\beta_{22} = 2.5$, and $\alpha = 0.01$. (b) Asymptotic order parameter γ_1^* vs N; the straight line has slope $-\mu = -0.32$. (c) Saturation time t^* vs N. The straight line has slope $\nu = 1.77$.

inside the square brackets in (1)], we estimate $\lambda = 0.18 \pm 0.02$. These data, not shown, will be reported elsewhere. More surprisingly, a first series of runs in three dimensions show similar behavior, with λ of the same order of magnitude (inset in Fig. 2). This said, the estimated value of the coarsening exponent λ is rather unusual. Even though $\lambda = 0.18$ is probably a lower bound (some of the data in Fig. 2 can be fitted to $\lambda = 0.2$ or 0.22), it certainly differs from $\frac{1}{3}$, the value expected for grain growth in binary alloys or other conserved order parameter systems [23], as well as from $\frac{2}{3}$, expected for spinodal decomposition in three-dimensional systems with hydrodynamic couplings [24]. The scaling behavior of γ_1^* with N, controlled by μ, is *not* a simple geometric consequence of the relative decrease of cells at a circular endoderm-ectoderm interface with N, since that would lead to $\gamma_1^* \sim N^{-(1/2)}$. At the moment, we have no satisfactory understanding of the recorded scaling laws.

In summary, we introduced a self-propelled particle model for cohesive cell rearrangements, with a velocity-dependent interaction term, which constitutes an alternative to the GGH model. Regarding the regeneration of *Hydra*, our model corroborates the experimental facts, as described in Ref. [7]. Our approach allows us to separately investigate the effects of random and coherent cell motion events. We have shown that even weak coherent motility facilitates cell sorting. Remarkably, we have found phase-ordering processes governed by power laws when velocity-dependent coupling is high enough, in contrast with the logarithmic behavior advocated for the GGH model [9]. There are two ways out of this contradiction: Either the GGH model does, in fact, exhibit algebraic scaling but was never explored in large-enough systems over long-enough times to reveal it, or it does show logarithmic decay asymptotically, but then, as hinted by our own results, this behavior is not robust to the presence of even the smallest amount of active coordinated motion between neighboring cells.

In this context, more extensive simulations of the GGH model are needed, as well as large-scale quantitative experiments, to find out which type of scaling laws actually governs cell sorting and, if power laws are found, to check whether the rather robust but unusual exponent values found in this work hold. More generally, the versatility and numerical efficiency of our approach could be useful in other situations where cohesive biological cells actively move coherently, such as wound healing, tumor growth, or early stages of development like gastrulation. Finally, biological cells interact via many channels and not only by contact adhesion. Some of these interactions (e.g., chemically mediated) are likely to be long-range, a feature which could potentially alter the scaling laws described here and deserves further investigation.

H. C. was funded in part by the EU Starflag and the French ANR Morphoscale projects. J. B., G. T., L. B., and R. A. thank the Brazilian agencies CNPq, Capes, and Fapergs.

[1] S. G. Lenhoff, *Hydra and the Birth of Experimental Biology-1744* (Boxwood Press, Pacific Grove, 1986); H. V. Wilson, J. Exp. Zool. **5**, 245 (1907); J. Holtfreter, Rev. Can. Biol. **3**, 220 (1944); A. Moscona, Exp. Cell Res. **3**, 535 (1952); J. P. Trinkaus and P. W. Groves, Proc. Natl. Acad. Sci. U.S.A. **41**, 787 (1955).
[2] M. S. Steinberg, Science **141**, 401 (1963).
[3] R. A. Foty, G. Forgacs, C. M. Pfleger, and M. S. Steinberg, Phys. Rev. Lett. **72**, 2298 (1994); C. Norotte *et al.*, Europhys. Lett. **81**, 46 003 (2008).
[4] M. Sato-Maeda, M. Uchida, F. Graner, and H. Tashiro, Dev. Biol. **162**, 77 (1994).
[5] J. C. M. Mombach, J. A. Glazier, R. C. Raphael, and M. Zajac, Phys. Rev. Lett. **75**, 2244 (1995).
[6] H. M. Phillips and M. S. Steinberg, J. Cell Sci. **30**, 1 (1978).
[7] J. P. Rieu, N. Kataoka, and Y. Sawada, Phys. Rev. E **57**, 924 (1998).
[8] J. P. Rieu *et al.*, Biophys. J. **79**, 1903 (2000).
[9] F. Graner and J. A. Glazier, Phys. Rev. Lett. **69**, 2013 (1992); J. A. Glazier and F. Graner, Phys. Rev. E **47**, 2128 (1993).
[10] N. J. Savill and P. Hogeweg, J. Theor. Biol. **184**, 229 (1997); A. F. M. Marée and P. Hogeweg, Proc. Natl. Acad. Sci. U.S.A. **98**, 3879 (2001).
[11] W.-J. Rappel, A. Nicol, A. Sarkissian, H. Levine, and W. F. Loomis, Phys. Rev. Lett. **83**, 1247 (1999).
[12] D. A. Beysens, G. Forgacs, and J. A. Glazier, Proc. Natl. Acad. Sci. U.S.A. **97**, 9467 (2000).
[13] T. T. Maeda *et al.*, BMC Syst. Biol. **41**, 1 (2007).
[14] See, e.g., I. D. Couzin *et al.*, J. Theor. Biol. **218**, 1 (2002); I. D. Couzin and J. Krause, Adv. Stud. Behav. **32**, 1 (2003).
[15] X.-L. Wu and A. Libchaber, Phys. Rev. Lett. **84**, 3017 (2000); G. Grégoire, H. Chaté, and Y. Tu, Phys. Rev. Lett. **86**, 556 (2001); Phys. Rev. E **64**, 011902 (2001).
[16] E. Ben-Jacob *et al.*, Phys. Rev. Lett. **75**, 2899 (1995); I. G. Ron, I. Golding, B. Lifsitz-Mercer, and E. Ben-Jacob, Physica (Amsterdam) **320A**, 485 (2003); I. Golding, I. Cohen, and E. Ben-Jacob, Europhys. Lett. **48**, 587 (1999); E. Ben-Jacob, Contemp. Phys. **38**, 205 (1997); E. Ben-Jacob, I. Cohen, and H. Levine, Adv. Phys. **49**, 395 (2000).
[17] B. Szabó *et al.*, Phys. Rev. E **74**, 061908 (2006).
[18] H. Gruler, U. Dewald, and M. Eberhardt, Eur. Phys. J. B **11**, 187 (1999).
[19] T. Vicsek, A. Czirok, E. Ben-Jacob, I. Cohen, and O. Shochet, Phys. Rev. Lett. **75**, 1226 (1995).
[20] G. Grégoire, H. Chaté, and Y. Tu, Physica (Amsterdam) **181D**, 157 (2003).
[21] G. Grégoire and H. Chaté, Phys. Rev. Lett. **92**, 025702 (2004).
[22] F. Family and T. Vicsek, J. Phys. A **18**, L75 (1985).
[23] G. F. Mazenko, Phys. Rev. B **43**, 8204 (1991).
[24] J. E. Farrell and O. T. Valls, Phys. Rev. B **40**, 7027 (1989).